Nano-Sized Polycrystalline ZSM-5 Aggregates Induced by Seeds in an Organic-Free Synthesis System

Xuchang Wang , Zhuo Ji , Qirui Jiao , Chuyu Jiao , Xiaosen Ma , Quanhua Wang , Jiajun Zheng * , Lichen Zhang , Yanchao Liu , Wenlin Li , Ruifeng Li *

Posted Date: 18 May 2023

doi: 10.20944/preprints202305.1272.v1

Keywords: ZSM-5; Polycrystalline aggregates; Nanosized crystal; Crystal seeds; Structure-directing agent

Article

Nano-sized polycrystalline ZSM-5 aggregates induced by seeds in an organic-free synthesis system

Xuchang Wang, Zhuo Ji, Qirui Jiao, Chuyu Jiao, Xiaosen Ma, Quanhua Wang, Jiajun Zheng *, Lichen Zhang, Yanchao Liu, Wenlin Li and Ruifeng Li *

College of Chemical Engineering and Technology, State Key Laboratory of Clean and Efficient Coal Utilization, Taiyuan University of Technology, Taiyuan 030024, China

* Correspondence: zhengjiajun@tyut.edu.cn (J.J.Z.); rfli@tyut.edu.cn (R.F.L.); Tel.:+86-03516018384

Abstract: Synthesis of ZSM-5 zeolite from OSDA-free systems has been a very interesting alternative method because it can avoid the usage of organic templates and consequent calcination step. However, in opened reports, organic substance such as alcohol is more or less involved. In the present work, a calcined commercial ZSM-5 zeolite was used as a seed, sodium aluminate as an aluminum source, silica sol as a silicon source, which ensures that there is no any organics (template) in the synthesis system, and polycrystalline ZSM-5 aggregates consisting of rod-like nanocrystals are successfully prepared in a completely OSDA-free system. The effects of seed (chemical component, dosage) and crystallization conditions on the synthesis of ZSM-5 were systematically investigated. The results show that highly crystallinity ZSM-5 aggregate consisting of primary nano-sized crystals with a size of less than 100 nm can be yielded from a gel precursor with 5.6 wt.% seed after hydrothermal treatment for 48 h. The results also shows that the chemical composition of the seeds had little effect on the topological structure and pore structure of the synthesized samples, but the seed with a low Si/Al ratio is more conducive to the rapid crystallization of zeolite and to the improvement of the acid, especially the strong acid centers of the catalyst.

Keywords: ZSM-5; Polycrystalline aggregates; Nanosized crystal; Crystal seeds; Structure-directing agent

1. Introduction

ZSM-5 is a typical microporous zeolite with a three-dimensional ordered double-10-membered rings channel structure. Where, the diameter of "Z" shaped pore is about 0.53 nm × 0.56 nm, and the diameter of the rectilinear elliptical pore perpendicular to "Z" shaped one is about 0.51 nm × 0.55 nm. The two kinds of pore cross each other, and the aperture at the intersection is about 0.9 nm. As a solid-acid catalyst, ZSM-5 zeolite has been widely used in petrochemical industry. For example, in the field of FCC catalysis, ZSM-5, as an active component, can significantly increase the olefin/oil ratio in products [1]. Most of the zeolite were reported to be prepared by using organic structure-directing agent (OSDA) as templates, which is usually used to direct the formation and to help stability of the zeolite framework. As OSDA, the most representative would be tetrapropylammonium cation, either in the form of its hydroxide (TPAOH) or in the form of a salt, preferably the bromide (TPABr), or a mixture of salt and hydroxide. The conventional method involving the synthesis of ZSM-5 zeolite is usually realized with the help of OSDA, which will waste resources, consume energy and pollute environment [2]. As a consequence, it has become extremely desired to develop an eco-friendly method for synthesizing ZSM-5 without organic templates.

Synthesis of zeolite crystals from an OSDA-free system has been a very interesting alternative method because it avoids using organic templates and consequent calcination step. In general, OSDA often plays important roles in directing crystallization and filling micropores. In recent years, an OSDA-free synthesis of zeolites with the help of zeolite seeding has been successfully developed. Here, the zeolite seed play a similar role to the OSDA for directing zeolite crystallization from the amorphous precursor. Consequently, researchers have devoted themselves to synthesizing highly crystalline ZSM-5 in the absence of organic templates [3–11]. For instance, Micro-scale, submicron-

scale and nano-scale ZSM-5 yielded from a template-free system was reported to be prepared in an environment friendly seed-assisted one-step method [2]. Hierarchical ZSM-5 zeolite composed of nanocrystals was also synthesized by template-free seed-assisted technique in a gel precursor with ethanol and using aluminum isopropoxide as Al-species and tetraethoxysilane (TEOS) as silicon-species [6]. MFI-SDS crystals were reported to be assembled from the rod-like nanocrystals with the same aligned direction in an OSDA-free synthesis system in the presence of the zeolite seeds[7]. For another example, nanocrystalline ZSM-5 was reported to be synthesized with the help of a seed suspension liquid obtained by dispersing the calcined seed in ethanol. However, in these synthesis, organic substance is more or less involved. For example, TEOS [6,7] as silicon resource, or $Al(O^iPr)_3$ [6,11] as aluminum resource, or crystals containing OSDA as seeds [2,8,10], or suspension seeds in ethanol [9–10] will inevitably bring organics especially alcohols in the synthesis system. The organic matter such as ethanol, which is the directly added or yielded from hydrolysis of raw materials in the synthesis system, may play a template by filling in the zeolite micropores [12–17] because of tetrahedron formed by ethanol and sodium ions, which can accelerate the nucleation and crystallization [12,13].

In the present work, a calcined commercial ZSM-5 zeolite was used as a seed, sodium aluminate as an aluminum source, silica sol as a silicon source, which ensures that there is no any organic substance (template) in the synthesis system, and polycrystalline ZSM-5 aggregates consisting of rod-like nanocrystals are successfully prepared in a completely OSDA-free system. The effects of the chemical component (Si/Al ratio) and the added amount of seeds, and crystallization time on the synthesis of ZSM-5 zeolite were investigated in detail.

2. Experimental Sections

2.1. Synthesis of Polycrystalline ZSM-5 Aggregates

ZSM-5 was prepared with the molar composition of the gel: $n(SiO_2)$: $n(Al_2O_3)$: $n(H_2O)$: $n(Na_2O)$=1 : 0.04 : 10 : 0.1. First, a certain volume of distilled water was measured, and then a certain mass of sodium aluminate (41 wt.% Al_2O_3, 35 wt.% Na_2O, Sinopharm Group) and sodium hydroxide (96 wt.%, Sinopharm Group) were added into the distilled water and stirred until the solution was clarified. Then, colloidal silica (40 wt.%, Qingdao Ocean Chemical Co. LTD) was dropwise added into the aforementioned solution followed by stirring at room temperature for about 5 min. Subsequently, crystal seed (NK-18, SiO_2/Al_2O_3 =18; NK-27, SiO_2/Al_2O_3 =27; NK-200, SiO_2/Al_2O_3 =200, Nankai University) after calcined at 550°C for 6 h in air was added and stirred for 4 h. The obtained gel precursor was transferred to a hydrothermal reactor lined with polytetrafluoron and crystallized for a certain time at 160°C. After crystallization, the zeolite was washed to neutral with deionized water, and the samples were named as Z5*n*-*x*-*y*. Here, the "*n*", "*x*", and "*y*" are the crystal seed (=18, 27, 200), added amount of seed ($x = m_{seed}/(m_{SiO_2} + m_{Al_2O_3})$), and crystallization time (h), respectively.

All of the as-synthesized Na-zeolite samples were calcined in muffle furnace with air atmosphere at 550 ℃ for 6 h, and the ammonium-formed sample was then acquired by exchanging with an 1 mol/L ammonium chloride solution with a solid-liquid ratio of 1: 20 for three times, 60 ℃, and each time for 2 h. After drying, the ammonium-formed zeolite samples were calcined at 550 ℃ in muffle furnace for 6 h so as to offer H-formed zeolite catalysts.

2.2. Characterization

X-ray powder diffraction (XRD) spectra were measured in the 2θ range from 5° to 50° with a scanning speed of 4°/min on a Shimadzu XRD-6000 diffractometer using Cu Kα radiation (λ = 1.5406 Å) operated at 40 kV and 30 mA. The relative crystallinity (RC) was calculated by comparing the peak areas of XRD diffraction between 2θ = 22.5 ~ 25° of the as-synthesized samples with those of Z518-5.6-48. The particle sizes and morphologies of the samples were performed on a Hitachi S4800 scanning electron microscopy (SEM). Transmission electron microscopy (TEM) was recorded on a JEM-2100F with an accelerating voltage of 200 kV. FT-IR spectra of zeolite framework vibration were

 doi:10.20944/preprints202305.1272.v1

measured using a Shimadzu FTIR-8400 spectrometer. N_2 adsorption/desorption isotherms at -196 ℃ were carried out on a NOVA 1200e sorption analyzer after the samples were activated at 300 ℃ under vacuum for 3 h. The pore size distribution curve was determined based on the Barrett-Joyner-Halenda (BJH) mode with the adsorption branch of the isotherm. The microporous surface area (S_{mic}), microporous volume (V_{mic}), and external surface area (S_{ext}) were calculated from the BJH method. Temperature-programmed desorption of ammonia (NH_3-TPD) was carried out on an AutochemΠ 2920 apparatus equipped with a thermal conductivity detector (TCD). ~20 mg of catalyst was loaded in a U-model quartz tube and supported by quartz wool. Then, it was treated at 550 ℃ for 3 h in a highly purified He (99.999%) flow. After cooling down to 120 ℃, the sample was saturated with a NH_3 (15 %)/He gas mixture, followed by purging with the highly purified He at 120 ℃ for an hour. Then, the temperature was increased at a rate of 10 ℃/min in a highly purified He flow (30 mL/min), and desorption of NH_3 was monitored. In this experiment, a water trap was set up between the sample and the TCD to avoid the influence of water.

3. Results and Discussion

Figure 1 is XRD pattern of the as-synthesized samples with different added amount of the seeds. The diffraction peaks at 7.88°, 8.76°, 23.0°, 23.84°, and 24.3° can be ascribed to the characteristic diffraction peaks of MFI topology (JCPDS: 44-00033) [2,3,5–10]. It can be seen that the added amount of the crystal seed plays an important role in the formation of ZSM-5 zeolite. A gel precursor without seed only generates an amorphous phase in the as-synthesized sample Z518-0-48. When the added amount of seed is lower than 2.8 wt.%, except for the characteristic diffraction peaks of MFI topological structure, two obvious diffraction peaks at 6.5° and 9.8° attributing to MOR zeolite emerge in the as-prepared sample Z518-2.8-48, suggesting that the sample Z518-2.8-48 mainly consisting of MFI topological structure mingled with a little of MOR can be obtained. It can be inferred from Figure 1 that about 5.6 wt.% seed added in the gel precursor is enough to induce in pure and high crystallization ZSM-5 zeolite. Figure 1 also displays that when seed amount is further increased from 5.6 wt.% to 11.2 wt.%, the as-synthesized sample Z518-11.2-48 has the similar while slightly intense characteristic diffraction peaks to the sample Z518-5.6-48 (Figure 1). The above result also suggests that the further increased amount of the seed has little effect on the topological structure of the as-synthesized samples.

As shown in Figure S1A1-A2, the SEM image of NK-18 suggests that the initial ZSM-5 serving as the seed is mono-dispersed single crystal with a size of about 1-2 μm. It can be seen from Figure 2 and Figure S1 that the added amount of the crystal seed strongly affects the formation and the morphology of the as-made samples. As shown in Figure 2 that the morphology of the as-prepared samples is very different from that of the seed crystals. The as-synthesized sample Z518-0-48 yielded from a gel precursor without any seed displays a worm-like monolith (Figure 2A), agree with the result of XRD as shown in Figure 1 very well. A precursor with an appropriate amount of seed gives the as-prepared samples with a polycrystalline morphology. As exhibited in Figure 2B-D, all the samples Z518-2.8-48, Z518-5.6-48, and Z518-11.2-48 display polycrystalline aggregates, which further consist of loosely aggregating primary nanocrystals with an estimated size of about less than 100 nm (Figure S2). As shown in Figure 2B, some plate-like crystals (the part rendered in red) can be found, which may be the impure MOR zeolite, which is in agreement with the above XRD result. No any amorphous form can be obviously detected in Z518-2.8-48, Z518-5.6-48, and Z518-11.2-48 samples, suggesting that the appropriately added amount of the seed can promote the as-synthesized sample to be highly crystalline and avoid the formation of amorphous form and impure MOR phase. As shown in Figure S3, both of the sample Z518-5.6-48 and Z518-11.2-48 have the similar N_2 adsorption-desorption isotherms with a combination of type-I and type-IV, indicating that the coexistence of the micropore and mesopore. The corresponding BJH pore size distribution curve of samples shows that a mesopore distribution ranging from 5 to 50 nm can be found in the two samples, which can be ascribed to the intercrystalline mesopore structure resulted from the loosely aggregating primary nanocrystals in the polycrystalline aggregates as shown in Figure S2. The N_2 adsorption data as shown in Table S1 shows that the Z518-5.6-48, and Z518-11.2-48 samples have the similar porosity

Preprints (www.preprints.org) | NOT PEER-REVIEWED | Posted: 18 May 2023 doi:10.20944/preprints202305.1272.v1

structure and crystalline, may also suggest that the further increased amount of the seed from 5.6 % to 11.2 % has little effect on the porosity structure and the elevated crystalline of as-synthesized samples.

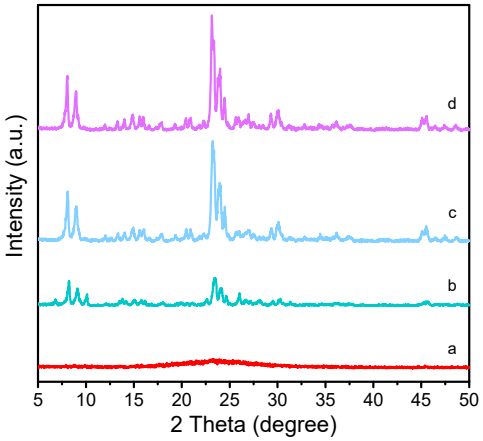

Figure 1. XRD pattern of the as-synthesized samples with different added amount of the seeds. a: Z518-0-48; b: Z518-2.8-48; c: Z518-5.6-48; d: Z518-11.2-48.

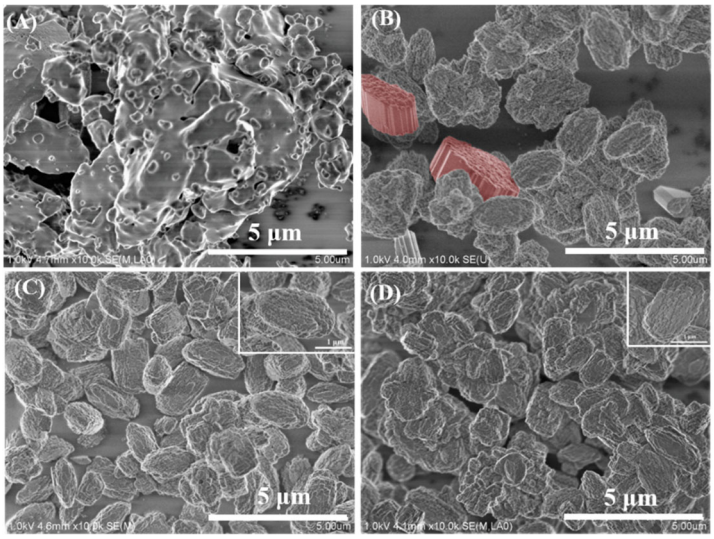

Figure 2. SEM images of as-synthesized samples with different amount of added seeds. (A): Z518-0-48; (B): Z518-2.8-48; (C): Z518-5.6-48; (D): Z518-11.2-48. The part rendered in red may be MOR zeolite.

XRD pattern of the as-made samples yielded from the same gel precursor with different crystallization time and the corresponding crystallization kinetic curve of the as-synthesized samples are shown in Figure 3. The characteristic diffraction peaks at 2θ = 7.9°, 8.8° and 23° in sample Z518-5.6-0 can be attributed to the influence of ZSM-5 seed in the precursor, indicating that ZSM-5 crystal seeds can remain relatively stable during the preparation of gel precursor. The main reason is that the Si/Al ratio of seed NK-18 is relatively low, and the zeolite framework with negative charge has electron repulsion on OH^-. In the alkaline environment, the Al atom in the framework will protect the nearby Si atom from the nucleophilic attack of hydroxide ions, thus forming the protective barriers for Si-species [19, 20]. When 0 h< "t" (the crystallization time) <12 h, the characteristic diffraction peaks attributed to MFI topological structure in the synthesized samples Z518-5.6-4, Z518-5.6-48 and Z518-5.6-12 gradually increase with the prolonged crystallization time (Figure 3A), while the corresponding relative crystallinity of the as-prepared samples such as Z518-5.6-12 is still low (<20%, Figure 3B), indicating that the synthesis gel system is still in the nucleation induction stage [21]. When the crystallization time "t" ≥ 14 h, the characteristic diffraction peaks of the as-synthesized

Preprints (www.preprints.org) | NOT PEER-REVIEWED | Posted: 18 May 2023 doi:10.20944/preprints202305.1272.v1

samples increase sharply (Figure 3A), and the relative crystallinity of corresponding sample Z518-5.6-14 reaches about 92 % of the sample Z518-5.6-48 (Figure 3B).

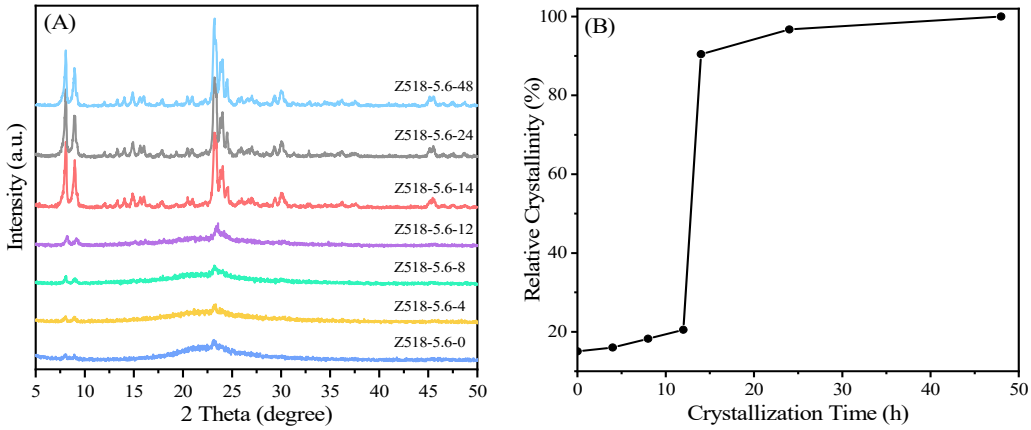

Figure 3. XRD pattern of the as-synthesized samples with the different crystallization time (A) and the corresponding crystallization kinetic curve (B).The relative crystallinity (RC) was calculated by comparing the peak areas of XRD diffraction between 2θ = 22.5 ~ 25° of the as-synthesized samples with those of sample Z518-5.6-48.

As shown in **Figure 4**, all of the samples yielded from the same gel precursor with the different crystallization time exhibit the characteristic vibration bands of MFI topological structure. For example, the absorption bands near 453 cm^{-1}, 553 cm^{-1} and 790 cm^{-1} belong to the internal framework vibration, the double five-member ring vibration and the asymmetric stretching of the AlO_4 and SiO_4 tetrahedron of ZSM-5 zeolite, respectively. It was reported that the ratio of the absorption band strength of 553 cm^{-1} to that of 453 cm^{-1} could be used to evaluate the degree of crystallization of the samples [22]. It can be inferred from Figure 4A that with the extended crystalline time, the relative degree of crystallinity of the as-synthesized samples gradually increase. This is consistent with the results as shown in Figure 3B. In addition, the asymmetric stretching vibrations of TO_4 (T = Si or Al) at 1090 cm^{-1} is closely related to the Si/Al ratio of the zeolite framework, and the increased Si/Al ratio will cause the vibration moving towards a high wavenumber. It can be inferred from Figure 4B that the prolonged crystalline time causes the asymmetric stretching vibrations of TO_4 to move towards the low wavenumber, may mean that with a prolonged crystalline time, more Al-species are inserted into the zeolite framework, which offers the as-synthesized samples with the decreased Si/Al ratios.

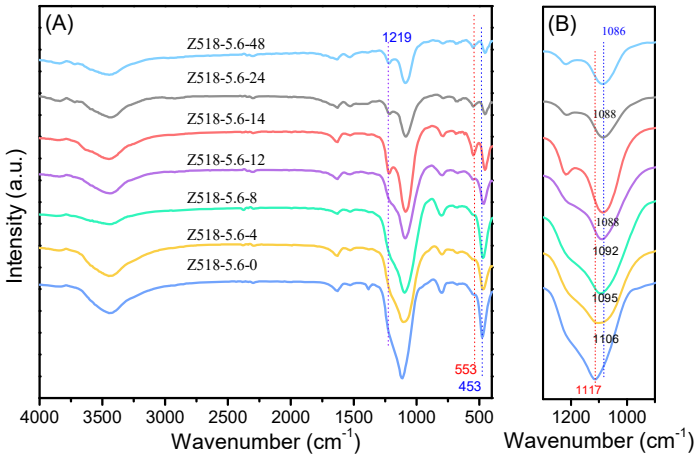

Figure 4. FT-IR spectra of as-synthesized samples generated from the same gel precursors with different crystallization time.

As shown in Figure 5, The shorter crystalline time such as less than 8 h, amorphous phase is detected to be the main body in the as-prepared samples. When the crystalline time is longer than 14

 doi:10.20944/preprints202305.1272.v1

h, all the crystals in the as-synthesized samples Z518-5.6-14, Z518-5.6-24 and Z518-5.6-48 have the similar polycrystalline morphology composed of primary nanocrystals, and no any amorphous phase can be obviously observed, agreeing with the results as shown in Figure 3 very well. It can be seen from Figure 5 I-J that the crystals in the as-synthesized sample Z518-5.6-48 are polycrystalline aggregates consisting of the rod-like nanocrystals estimated at about less than 100 nm in diameter. The TEM image of sample Z518-5.6-48 also shows that some of the crystals in the as-synthesized may have a core-shell structure: a monocrystal core warped by a polycrystalline shell, which makes the as-synthesized crystals seeming more like a polycrystalline aggregate.

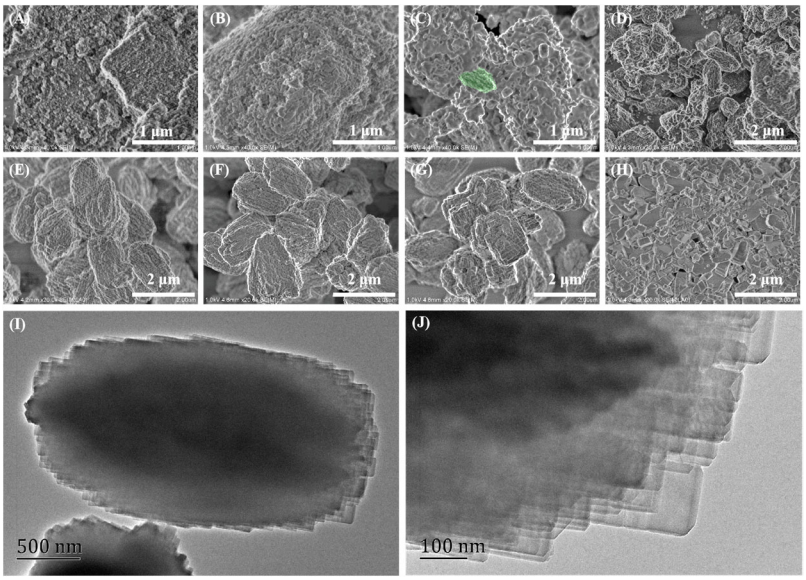

Figure 5. SEM and TEM images of the as-synthesized samples with different crystallization time. SEM images of (A): Z518-5.6-0; (B): Z518-5.6-4; (C): Z518-5.6-8; (D): Z518-5.6-12; (E): Z518-5.6-14; (F): Z518-5.6-24; (G): Z518-5.6-48; (H): NK-18; TEM images of (I) and (J): Z518-5.6-48.

The formation process of the as-prepared polycrystalline aggregates can be summarized as follows: Despite the commercial ZSM-5 (NK-18) has a low framework Si/Al ratio, which ensures NK-18 zeolite acting as the crystal seed to remain a relatively stable during the preparation of gel precursor [19,20]. While, in the subsequent hydrothermal synthesis process, it is inevitable that the ZSM-5 crystal seeds are partially dissolved by the alkaline gel precursor. The dissolved crystal seeds will release abundant primary/secondary structural units, which contributes to stimulating an explosive nucleation and results in the formation of a large number of nanocrystals [23]. During the hydrothermal crystallization, zeolite seeds along with the primary/secondary structural units resulted from partially dissolved seeds play the similar role to OSDA for directing zeolite crystallization from the amorphous gel precursors. Due to the high surface energy, the nanocrystals caused by the explosive nucleation in a short time are highly unstable. In order to decrease the surface energy, the nanocrystals will suffer from interattraction and then form polycrystalline aggregates by self-assembly [6–7,17], or be adsorbed on the external surface of the reserved seed crystals and form the polycrystalline aggregates with the reserved seed crystal as cores and rod-like nanocrystals as polycrystalline shell [24].

Figure 6 is the N_2 adsorption-desorption isotherms and the corresponding BJH pore size distribution curves. It can be seen from Figure 6A that the N_2 adsorption isotherm curves exhibit a steep increase at the relative pressure $p/p_0 < 0.02$ and a hysteresis loop at a relative pressure p/p_0 of 0.45-0.8, indicating the co-existence of intrinsic micropores and meso- or/and macropores in the samples. The hysteresis loop at a relative pressure p/p_0 of 0.45-0.8 can be attributed to the capillary condensation [17] in open mesopores or macropores obtained by filling the interparticles spaces of primary MFI zeolite in the aggregates. Moreover, hysteresis loops at $p/p_0>0.8$ are present in the nitrogen isotherm of samples especially Z518-5.6-4 yielded from a shorter crystalline time, which can

Preprints (www.preprints.org) | NOT PEER-REVIEWED | Posted: 18 May 2023 doi:10.20944/preprints202305.1272.v1

be caused by the macropores in the worm-like amorphous phase as shown in Figure 5B. The BJH pore structure distribution calculated from the adsorption branch of the isotherms are shown in Figure 6B. Samples Z518-5.6-14, Z518-5.6-24 and Z518-5.6-48 have an obvious mesopore distribution centering at about 15 nm, attributing to the intercrystalline mesopores between the primary MFI crystals in the aggregates [6–8,11]. Larger pore distribution centering at about more than 100 nm detected in the samples Z518-5.6-4 and Z518-5.6-8 can be ascribed to the macropores in the worm-like amorphous phase (Figure 5B-C). As shown in Table 1, with the prolonged hydrothermal treatment time, the microporous properties such as microporous areas (S_{mic}), microporous volume (V_{mic}) display a continuously increased trend, suggesting a progressively increased "RC", which is in agreement with the result as shown in Figure 3B.

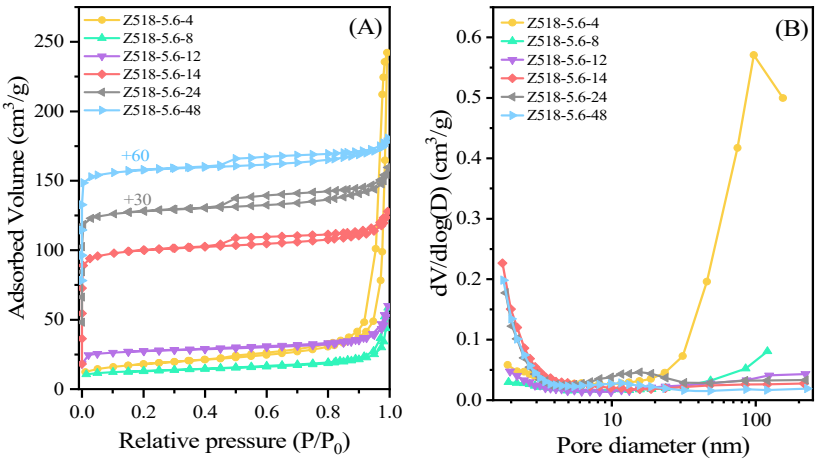

Figure 6. N_2 adsorption-desorption isotherm and the corresponding BJH pore size distribution curves of the as-synthesized samples generated from the same gel precursor treated with different time.

Table 1. Textural properties of the as-synthesized samples with different crystallization time.

Sample	S_{BET} (m^2/g)	S_{mic} (m^2/g)	S_{ext} (m^2/g)	V_{total} (cm^3/g)	V_{mic} (cm^3/g)	V_{ext} (cm^3/g)	[1]RC (%)
Z518-5.6-4	66	13	51	0.375	0.002	0.373	16.0
Z518-5.6-8	48	26	22	0.089	0.009	0.080	18.2
Z518-5.6-12	105	84	21	0.093	0.031	0.062	20.5
Z518-5.6-14	396	355	41	0.198	0.134	0.064	90.4
Z518-5.6-24	390	351	40	0.200	0.131	0.069	96.7
Z518-5.6-48	392	351	41	0.213	0.132	0.081	100

[1] The relative crystallinity (RC) is the crystallinity of the as-synthesized samples to the one of the reference Z518-5.6-48. That is calculated by comparing the peak areas of XRD diffraction between 2θ = 22.5 ~ 25° of the as-synthesized samples with those of sample Z518-5.6-48.

In order to investigate the effect of the chemical component of the seed on the synthesis of ZSM-5, seeds such as NK-18, NK-27, NK-200 with different Si/Al ratio were used for preparing ZSM-5 in an organic-templates-free system. It can be inferred from Figure S4A that the chemical component of the seeds has little effect on the synthesis of pure phase ZSM-5 zeolite. All the samples Z518-5.6-48, Z527-5.6-48 and Z5200-5.6-48 have the similar characteristic diffraction peaks attributing to MFI topological structure while with a slightly weakened peak intensity with the increased Si/Al ratios of the used seeds (Figure S4A). It can be seen from Figure S4B that the samples induced by the different seeds have the similar N_2 adsorption-desorption isotherm, and the microporous properties of the as-synthesized samples display a slightly and expressively decreased trend with enhanced Si/Al ratios of the used seeds (Table 2). The above result means that low Si/Al ratios seeds may be in favor of directing and promoting a fast crystallization of zeolites. It can be seen from Figure S5 that the samples Z527-5.6-48 and Z5200-5.6-48 induced by the different seeds of NK-27 and NK-200 have the similar polycrystalline aggregates to the Z518-5.6-48, rather different from the corresponding seeding

crystals (Figure S1), and no any amorphous phase can be found in the as-synthesized samples. Element analysis decided by EDS is displayed in Figure S6, Combining with the result as shown in Table 2, the seeds with the different Si/Al ratios has a little effect on the chemical component of the as-synthesized ZSM-5 samples, and all the samples have the similar Si/Al ratio of about 11.3-11.6, much lower than those of the used seeds. As shown in Figure S7, all of the samples Z518-5.6-48, Z527-5.6-48 and Z5200-5.6-48 display the similar NH_3-TPD curves. In order to determine the acid amount, NH_3-TPD curves were carried out peak-differentiating and fitting, and shown in Figure S8. It can be seen that all of the acid sites of the as-synthesized samples induced by the seeds with different Si/Al ratios can be fitting into weak acid, moderate-strength acid, and strong acid centers [8,17]. It can be seen from Table 2. that the three samples have the comparable acid density except Z518-5.6-48 yielded from the gel precursors with low Si/Al ratio seeds has more strong acid sites than the samples Z518-5.6-48 and Z527-5.6-48 induced by seeds with relatively high Si/Al ratios.

Table 2. Physical and chemical properties of the samples yielded from the similar gel precursors induced by a crystal seed with different Si/Al ratios.

Sample	S_{BET} (m^2/g)	Smic (m^2/g)	V_{total} (cm^3/g)	V_{mic} (cm^3/g)	[1]RC (%)	[2]Si/Al	Acid amount (μmol/g)			
							weak	medium	strong	total
Z518-5.6-48	392	352	0.186	0.130	100	11.3	218	65	293	576
Z527-5.6-48	376	333	0.185	0.123	99	11.3	212	83	224	519
Z5200-5.6-48	356	314	0.193	0.117	99	11.6	205	79	221	505

[1] the relative crystallinity (RC) is the crystallinity of the as-synthesized samples to the one of the reference Z518-5.6-48. That is calculated by comparing the peak areas of XRD diffraction between 2θ = 22.5 ~ 25° of the as-synthesized samples with those of sample Z518-5.6-48. [2] was determined by EDS analysis.

4. Conclusions

A polycrystalline ZSM-5 aggregates were synthesized by a sol-gel system in the absence of any organics. The seeds played a crucial role in directing zeolite crystallization from the amorphous precursor and accelerating the nucleation and crystallization. About 5.6 wt.% calcined seed added in the gel precursor is enough to induce in a pure and high crystallization ZSM-5 zeolite, while excessively low seed resulted in an amorphous phase or a sample represented by ZSM-5 mingled with a little MOR phase. The chemical component of the seeds has a slight effect on the synthesis of pure phase ZSM-5 zeolite, and a low Si/Al ratio seed was in favor of directing the formation and crystallization of ZSM-5 zeolites with a relatively high degree of crystallinity and more strong acid sites. This research provides a simple and feasible approach to realizing the prepare of zeolite in a true OSDA-free system.

Supplementary: Table S1. Pore structure parameter and relative crystallinity of the as-synthesized samples; Figure S1. SEM images of the crystals seeds, (A1) and (A2): NK-18,(B1) and (B2): NK-27, (C1) and (C2): NK-200; Figure S2. SEM images of (A) and (B): Z518-2.8-48; (C): Z518-5.6-48; (D): Z518-11.2-48; Figure S3. N_2 adsorption-desorption isotherm (A) and the corresponding BJH pore size distribution curves (B) of the as-synthesized samples; Figure S4. XRD pattern (A) and N_2 adsorption-desorption isotherm (B) of the samples prepared in a OSDA-free system induced by seeds with different Si/Al ratios; Figure S5. SEM images of the samples yielded from the similar gel precursors induced by seeds with different Si/Al ratios; Figure S6. EDS analysis of the as-synthesized samples induced by the seeds with different Si/Al ratios; Figure S7. NH_3-TPD profiles of samples induced by seeds with different Si/Al ratios; Figure S8. Peak-differentiating and fitting of the NH_3-TPD curves.

Author Contributions: Conceptualization, J.J.Z. and R.F.L.; methodology, J.J.Z.; validation, X.C.W. and Z.J.; formal analysis, L.C.Z. and Y.C.L.; investigation, Q.R.J., C.Y.J. and X.S.M.; resources, J.J.Z. and R.F.L.; data curation, X.C.W.; writing—original draft preparation, X.C.W.; writing—review

and editing, J.J.Z.; supervision, Q.H.W.; project administration, W.L. L., J.J.Z. and R.F.L.; funding acquisition, J.J.Z. and R.F.L.

Funding: This research was funded by the National Nature Science Foundation of China (Grant No. U19B2003, 21706177, 21975174), and China Petroleum & Chemical Corporation (121014-2).

Conflicts of Interest: The authors declare no conflict of interest.

References

1. Pan M, Zheng J J, Liu Y J, Ning W W, Tian H P, Li R F. Construction and practical application of a novel zeolite catalyst for hierarchically cracking of heavy oil. *J. Catal.* **2019**, *369*, 72–85. DOI: 10.1016/j.jcat.2018.10.032.
2. Wang J, Zhang R Z, Han L N, Wang J C, Zhao L F. Seed-assisted synthesis and characterization of nano and micron ZSM-5 molecular sieves in template-free system. *J. Solid State Chem.* **2020**, *290*, 121536–121547. DOI: 10.1016/j.jssc.2020.121536.
3. Lai R, Gavalas G R. ZSM-5 membrane synthesis with organic-free mixtures. *Microporous Mesoporous Mater.* **2000**, *38*, 239–245. DOI: 10.1016/s1387-1811(00)00143-8.
4. Wang Y Q, Wang X, Wu Q M, Meng X J., Jin Y Y, Zhou X Z, Xiao F S. Seed-directed and organotemplate-free synthesis of TON zeolite. *Catal. Today* **2014**, *226*, 103–108. DOI: 10.1016/j.cattod.2013.08.002.
5. Yue Y Y, Gu L L, Zhou Y N, Liu H Y, Yuan P, Zhu H B, Bai Z S, Bao X J. Template-free synthesis and catalytic applications of microporous and hierarchical ZSM-5 zeolites from natural aluminosilicate minerals. *Ind. Eng. Chem. Res.* **2017**, *56*, 10069–10077. DOI: 10.1021/acs.iecr.7b02531.
6. Shestakova D O, Babina K A, Sladkovskiy D A, Parkhomchuk E V. Seed-assisted synthesis of hierarchical zeolite ZSM-5 in the absence of organic templates. *Mater. Chem. Phys.* **2022**, *288*, 126432–126441. DOI: 10.1016/j.matchemphys.2022.126432.
7. Zhang H Y, Wang L, Zhang D L, Meng X J, Xiao F S. Mesoporous and Al-rich MFI crystals assembled with aligned nanorods in the absence of organic templates. *Microporous Mesoporous Mater.* **2016**, *233*, 133–139. DOI: 10.1016/j.micromeso.2015.11.063.
8. Gao Y, Wu G, Ma F W, Liu C T, Jiang F, Wang Y, Wang A J. Modified seeding method for preparing hierarchical nanocrystalline ZSM-5 catalysts for methanol aromatization. *Microporous Mesoporous Mater.* **2016**, *226*, 251–259. DOI: 10.1016/j.micromeso.2015.11.066.
9. Nada M H, Larsen S C. Insight into seed-assisted template free synthesis of ZSM-5 zeolites. *Microporous Mesoporous Mater.* **2017**, *239*, 444–452. DOI: 10.1016/j.micromeso.2016.10.040.
10. Hamidzadeh M, Saeidi M, Komeili S. Modified seeding method to produce hierarchical nanocrystalline ZSM-5 zeolite. *Mater. Today Commun.* **2020**, *25*, 101308. DOI: 10.1016/j.mtcomm.2020.101308.
11. Li Q, Cong W W, Xu C Y, Zhang S G, Wang F, Han D Z, Wang G J, Bing L C. New insight into the inductive effect of various seeds on the template-free synthesis of ZSM-5 zeolite. *CrystEngComm* **2021**, *23*, 8641–8649. DOI: 10.1039/d1ce01067k.
12. Feng F X, Dou T, Xiao Y Z, Cao J H. Effect of solvent on zeolite synthesis. *J. Energy Chem.* **1996**, 5, 351–356. DOI: 10.1016/S1003-9953-1996-5-4-351-356.
13. Zhang D S, Wang R J, Yang X X. Application of fractional factorial design to ZSM-5 synthesis using ethanol as template. *Microporous Mesoporous Mater.* **2009**, *126*, 8–13. DOI: 10.1016/j.micromeso.2009.03.015.
14. Ma T, Zhang L M, Song Y, Shang Y S, Zhai Y L, Gong Y J. A comparative synthesis of ZSM-5 with ethanol or TPABr template: distinction of Brønsted/Lewis acidity ratio and its impact on n-hexane cracking. *Catal. Sci. Technol.* **2018**, *8*, 1923–1935. DOI: 10.1039/c7cy02418e.
15. Uguina M A, Lucas A D, Ruiz F, Serrano D P. Synthesis of ZSM-5 from ethanol-containing systems. Influence of the gel composition. *Ind. Eng. Chem. Res.* **1995**, *34*, 451–456. DOI: 10.1021/ie00041a004.
16. Falamaki C, Edrissi M, Sohrabi M. Studies on the crystallization kinetics of zeolite ZSM-5 with 1,6-hexanediol as a structure-directing agent. *Zeolites* **1997**, *19*, 2–5. DOI: 10.1016/S0144-2449(97)00025-0.
17. Yang X N, Ma X S, Wang X C, Qin B, Zhang L C, Du Y Z, Liu Y C, Wang Q H, Wang Y, Zheng J J. Caterpillar-shaped hierarchical ZSM-5 resulted from the self-assembly of regularly primary nano-sized zeolite crystals. *J. Porous Mater.* DOI: 10.1007/s10934-023-01444-0.
18. Groen J C, Zhu W D, Brouwer S, Huynink S J, Kapteijn F, Moulijn J A, Pérez-Ramírez J. Direct demonstration of enhanced diffusion in mesoporous ZSM-5 zeolite obtained via controlled desilication. *J. Am. Chem. Soc.* **2007**, *129*, 355–360. DOI: 10.1021/ja065737o.
19. Zhang D Z, Jin C Z, Zou M M, Huang S J. Mesopore engineering for well-defined mesoporosity in Al-rich aluminosilicate zeolites. *Chem.–Eur. J.* **2019**, *25*, 2675–2683. DOI: 10.1002/chem.201802912.
20. Chen L H, Sun M H, Wang Z, Yang W M, Xie Z K, Su B L. Hierarchically structured zeolites: from design to application. *Chem. Rev.* **2020**, *120*, 11194–11294. DOI: 10.1021/acs.chemrev.0c00016.
21. Wang Y, Xiao F S. Understanding mechanism and designing strategies for sustainable synthesis of zeolites: A personal story. *Chem. Rec.* **2016**, *16*, 1054–1066. DOI: 10.1002/tcr.201500255.

22. Ravishankar R, Kirschhock C, Schoeman B J , Vanoppen P, Grobet P J, Storck S, Maier W F, Martens J A, Schryver F C, Jacobs P A. Physicochemical characterization of silicalite-1 nanophase material. *J. Phys. Chem. B* **1998**, *102*: 2633–2639. DOI: 10.1021/jp973147u.
23. Ning W W, Yang X N, Zheng J J, Sun X B, Pan M, Li R F. An environmentally friendly route to prepare hierarchical ZSM-12 using waste liquor as partial nutrients. *Mater. Chem. & Phy.*, 2019, *223*: 299–305. DOI: 10.1016/j.matchemphys.2018.10.069.
24. Wang H Q, Shen B Y, Chen X, Xiong H, Wang H M, Song W L, Cui C J, Wei F, Qian W Z. Modulating inherent lewis acidity at the intergrowth interface of mortise-tenon zeolite catalyst. *Nat. Commun.* **2022**, *13*, 2924–2932. DOI: 10.1038/s41467-022-30538-7.